Graphene Tunneling Transit-Time Terahertz Oscillator Based on Electrically Induced p–i–n Junction

Victor Ryzhii[1,2], Maxim Ryzhii[1,2], Vladimir Mitin[3], and Michael S. Shur[4]

[1]*Computational Nanoelectronics Laboratory, University of Aizu, Aizu-Wakamatsu, Fukushima 965-8580, Japan*
[2]*Japan Science and Technology Agency, CREST, Tokyo 107-0075, Japan*
[3]*Department of Electrical Engineering, University at Buffalo, State University of New York, NY 14260, U.S.A.*
[4]*Department of Electrical, Electronics, and System Engineering, Rensselaer Polytechnic Institute, Troy, NY 12180, U.S.A.*

Received February 4, 2009; accepted February 23, 2009; published online March 13, 2009

We propose and analyze a graphene tunneling transit time device based on a heterostructure with a lateral p–i–n junction electrically induced in the graphene layer by the applied gate voltages of different polarity. The depleted i-section of the graphene layer (between the gates) serves as both the tunneling injector and the transit region. Using the developed device model, we demonstrate that the ballistic transit of electrons and holes generated due to interband tunneling in the i-section results in the negative ac conductance in the terahertz frequency range, so that the device can serve as a terahertz oscillator.

DOI: 10.1143/APEX.2.034503

Graphene is considered as promising candidate for different future electronic and optoelectronic devices. Its most distinctive features beneficial for device applications include high electron and hole mobilities in a wide range of temperatures, the possibility of bandgap engineering (creation of the graphene-based structures with the energy gap from zero to fairly large values), formation of electrically induced lateral p–n junctions (see, for instance, refs. 1–5).

The operation of graphene field-effect transistors (G-FETs) is accompanied by the formation of the lateral n–p–n (or p–n–p) junction under the controlling (top) gate and the pertinent energy barrier.[6–9] The tunneling across such a n–p–n junction prevents the achievement of a low off-state current.[9] This limits possible realization of G-FETs in large scale digital electronic circuits and forces to consider the graphene structures in which the energy gap is reinstated (graphene nanoribbons and graphene bilayers with the energy gap open by the transverse electric field).[10–16]

Unique properties of graphene already produced not only using peeling technology but also epitaxial methods as well as graphene nanoribbons and bilayers, particularly, experimental evidences of the possibility of ballistic electron and hole transport in samples with several micrometer sizes even at room temperatures (see, for instance, refs. 17 and 18) stimulate inventions of different graphene-based devices which could not be realized the past using the customary materials.

In this paper, we propose a transit-time oscillator which can operate in the terahertz (THz) range of frequencies and substantiate the operational principle of the device. The operation of the device in question is associated with the tunneling electron injection in an electrically induced reverse biased lateral p–i–n junction and the electron and hole transit-time effects in its depleted section. In the following, we call this device is the graphene tunneling transit-time (G-TUNNETT) terahertz oscillator. The tunneling generation through the zero energy gap and propagation of electrons and holes with their directed velocity v_x close to the characteristic velocity $v_W \simeq 10^8$ cm/s of the graphene energy spectrum ($v_x \sim v_W$), can provides significant advantages of G-TUNNETTs in comparison with the existing and discussed TUNNETTs based on the conventional semiconductor materials (see, for instance, refs. 19 and 20 and the references therein). Using the developed device model, we calculate the high-frequency characteristics. The device under consideration comprises a graphene layer with the source and drain contacts and the gates. The lateral p–i–n junction can be formed by two top gates biased by the dc voltages V_p and V_n of different polarities ($V_p < 0$, $V_n > 0$). The G-TUNNETT structure under consideration and its band diagram (at the applied source–drain voltage V, so that the lateral p–i–n junction is reverse biased) are schematically shown in Figs. 1(a) and 1(b), respectively. It is assumed that apart from a dc component $V_0 > 0$ which corresponds to a reverse bias, the net source–drain voltage V comprises also an ac component $\delta V \exp(-i\omega t)$: $V = V_0 + \delta V \exp(-i\omega t)$, where δV and ω are the signal amplitude and frequency, respectively.

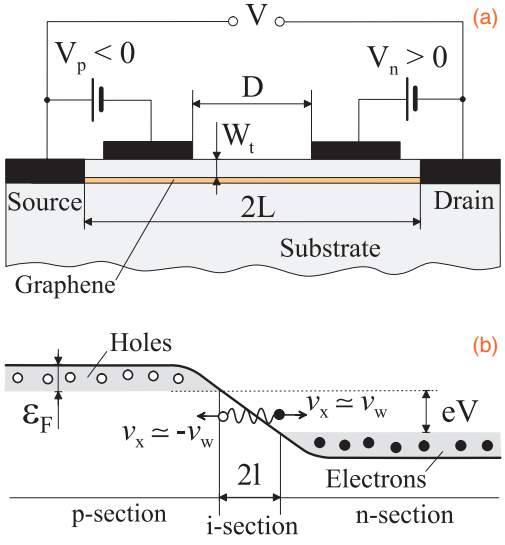

Fig. 1. Schematic view of a G-TUNNETT (a) structure and (b) its band diagram.

Thus, the graphene layer is partitioned into three sections: p- and n-sections adjacent to the source and drain contacts, respectively, and depleted section in the center (i-section). The depleted section of the graphene layer plays the dual role: (1) a strong electric field in the i-section provides the tunneling generation of electrons and holes and (2) this

section serves as the transit region where the generated electrons and holes propagating ballistically across this region induce the current in the p- and n-sections (as well as, possibly in the contacts) and, hence, the terminal current in the source–drain circuit. Considering for definiteness the "symmetric" device structure with $V_n = -V_p = V_t$) corresponding to Fig. 1, we shall calculate its source–drain ac conductance σ_ω^{sd} (dynamic conductance) as a function of the structural parameters and the signal frequency and demonstrate that $\sigma_\omega^{sd} < 0$ in certain (THz) frequency ranges.

Using the value of the interband tunneling probability,[5,21] and roughly estimating the electric field in the i-section as $\mathcal{E} \simeq V/2l$, where $2l$ is the length of the depleted i-section ($2l \simeq D$ if the spacing between the top gates $D \gg W_t$, were W_t is the thickness of the layers separating the graphene layer and the gates; more strict and detailed calculations can be found in refs. 21 and 22), for the rate of the tunneling generation of electron hole pair (per unit length in the transverse direction) in the i-section in the situation under consideration one can obtain

$$G \simeq \frac{g_0}{8\pi\sqrt{2e\hbar\, v_W l}}\, V^{3/2}. \tag{1}$$

Here $g_0 = 2e^2/\pi\hbar$, e is the electron charge, and $\hbar$ is the reduced Planck constant. This corresponds to the source–drain dc current

$$J_0 = 2eG_0 = \frac{g_0}{4\pi}\sqrt{\frac{e}{2\hbar\, v_W l}}\, V_0^{3/2}. \tag{2}$$

The ac component of the generation rate is given by

$$\delta G_\omega \simeq \frac{3g_0}{16\pi\sqrt{2e\hbar\, v_W l}}\, V_0^{1/2}\delta V_\omega = \frac{3}{2}\,\frac{J_0}{e}\,\frac{\delta V_\omega}{V_0}. \tag{3}$$

The tunneling probability w is a fairly sharp function of the angle between the direction of the electron (hole) motion and the x-direction (from the source to the drain): $w(\theta) \simeq \exp(-\alpha \sin^2\theta)$, where $\alpha \propto D$ is rather large.[5] Considering this, one can disregard some spread in the x-component of the velocity ($\Delta v_x/v_W \simeq 1/2\alpha$) of the injected electrons and assume that all the generated electrons and holes propagate in the x-direction with the velocity $v_x \simeq v_W$.

In the case of ballistic electron and hole transport in the i-section when the generated electrons and holes do not change the directions of their propagation, the continuity equations governing the ac components of the electrons and holes densities $\delta\Sigma_\omega^-$ and $\delta\Sigma_\omega^+$ can be presented as:

$$-i\omega\delta\Sigma_\omega^{\mp} \pm v_W\,\frac{d\delta\,\Sigma_\omega^{\mp}}{dx} = \frac{\delta G_\omega}{2l}, \tag{4}$$

The boundary conditions are as follows: $\delta\Sigma_\omega^{\mp}|_{x=\mp l} = 0$. Solving eq. (4) with these boundary conditions, we arrive at

$$\delta\Sigma_\omega^{\mp}(x) = \frac{\delta G_\omega}{2l}\cdot\frac{\exp[i\omega(l \pm x)/v_W] - 1}{i\omega} \tag{5}$$

Considering eqs. (4) and (5), for the net ac current $\delta J_\omega(x) = ev_W[\delta\Sigma_\omega^-(x) + \delta\Sigma_\omega^+(x)]$, created by both the generated electrons and holes, one can obtain

$$\delta J_\omega(x) = e\delta G_\omega\left[\frac{e^{i\omega\tau}\cos(\omega\tau\, x/l) - 1}{i\omega\tau}\right]. \tag{6}$$

Here, we have introduced the characteristic transit time $\tau = l/v_W$ Since the real time of the electron and hole transit across the i-section varies from 0 to $2l/v_W$, τ is actually the mean transit time. If the signal frequency ω is smaller than the plasma oscillations in the p- and n-sections Ω, ($\omega < \Omega$), these sections can be considered as just highly conducting electrodes, so that the terminal ac current is mainly induced in them. In this case, the ac component of the source–drain terminal current δJ_ω^{sd}, i.e., the ac current induced by the propagating electrons in the external circuit connecting the source and the drain can, according to the Ramo–Shockley theorem,[23,24] be presented as $\delta J_\omega^{sd} = \int_{-l}^{l} dx\, g(x)\delta J_\omega(x) - i\omega C\delta V_\omega$, where $g(x)$ is the form-factor determined by the shape of highly conducting regions (the p-section and the drain contact) and C is the i-section geometrical capacitance. The factor $g(x)$ is associated with different contributions to the induced current of the electrons and holes at different distances from the highly conducting regions. For the bulky conducting regions $g(x) \simeq 1/2l$, whereas for the blade-like conducting regions,[25] $g(x) = 1/\pi\sqrt{l^2 - x^2}$. For the i-section capacitance one can use the following formula:[26] $C = (\epsilon/4\pi^2)\ln(4L/l)$, where ϵ is the dielectric constant. Considering eq. (3), we arrive at the following formula for the ac conductance $\sigma_\omega^{sd} = \delta J_\omega^{sd}/\delta V_\omega$:

$$\sigma_\omega^{sd} = \frac{3\sigma_0}{2\pi}\int_{-1}^{1}\frac{d\xi}{\sqrt{1-\xi^2}}\left[\frac{e^{i\omega\tau}\cos(\omega\tau\xi) - 1}{i\omega\tau}\right] - i\omega\, C$$
$$= \frac{3\sigma_0}{2}\left[\frac{e^{i\omega\tau}\mathcal{J}_0(\omega\tau) - 1}{i\omega\tau}\right] - i\omega\, C, \tag{7}$$

where $\sigma_0 = J_0/V_0$ is the dc conductance and $\mathcal{J}_0(\xi)$ is the Bessel function. The real and imaginary parts of the ac conductance are given by

$$\mathrm{Re}\,\sigma_\omega^{sd} = \frac{3\sigma_0}{2}\,\frac{\sin(\omega\tau)}{\omega\tau}\,\mathcal{J}_0(\omega\tau), \tag{8}$$

$$\mathrm{Im}\,\sigma_\omega^{sd} = \frac{3\sigma_0}{2}\left[\frac{1 - \cos(\omega\tau)\mathcal{J}_0(\omega\tau)}{\omega\tau} - c\,\omega\tau\right], \tag{9}$$

where $c = 2C/3\sigma_0\tau$. At relatively low signal frequencies ($\omega\tau \ll 1$), eqs. (7) and (8) yield $\mathrm{Re}\,\sigma_\omega^{sd} \simeq (3\sigma_0/2)(1 - 7\omega^2\tau^2/12)$ and $\mathrm{Im}\,\sigma_\omega^{sd} \simeq (3\sigma_0)(3/4 - c)\omega\tau$, respectively. Thus, $\sigma_0^{sd} \simeq 3\sigma_0/2$, i.e., is equal to the differential dc conductance $\sigma_{diff}^{sd} = (\partial J_0/\partial V_0)|_{V_t=\mathrm{const}}$. Assuming that $2l = 0.5\,\mu$m, $2L = 2\,\mu$m, $\varepsilon = 3.8$, and $V_0 = 0.1$–1 V, we obtain $\sigma_0 \simeq (200$–$700)$ mS/mm and $c \simeq 0.34$.

The real part of the ac conductance $\mathrm{Re}\,\sigma_\omega^{sd}$ turns zero at the following signal frequencies $f = \omega/2\pi$: $f_1^- \simeq 0.38/\tau, f_1^+ = 0.5/\tau, f_2^- \simeq 0.88/\tau, f_2^+ = 1/\tau, \ldots$. In the frequency ranges $0.38/\tau < f < 0.5/\tau$ and $0.88/\tau < f < 1/\tau$, the real part of the ac conductance is negative. In particular, at $2l = 0.7\,\mu$m ($\tau = 0.35$ ps), $f_1^- \simeq 1.08$ THz and $f_1^+ = 1.43$ THz. The real part of the ac conductance $\mathrm{Re}\,\sigma_\omega^{sd}$ reaches minima at certain frequencies $f_1, f_2, \ldots$, which fall into the intervals $f_1^- < f_1 < f_1^+$, $f_2^- < f_2 < f_2^+, \ldots$. The quantity $\mathrm{Re}\,\sigma_\omega^{sd}$ increases with increasing source–drain voltage and, consequently, dc current. A decrease in the i-section length at fixed source–drain voltage gives rise to an increase both in $|\mathrm{Re}\,\sigma_\omega^{sd}|$ and in the frequencies $f_1, f_2, \ldots$, where $\mathrm{Re}\,\sigma_\omega^{sd}$ exhibits minima.

Figure 2 shows the real and imaginary parts of the ac conductance σ_ω^{sd} as functions of the signal frequency $f = \omega/2\pi$ calculated for $2l = 0.5\,\mu$m and $2l = 0.7\,\mu$m. The real part exhibits a pronounced oscillatory behavior with the

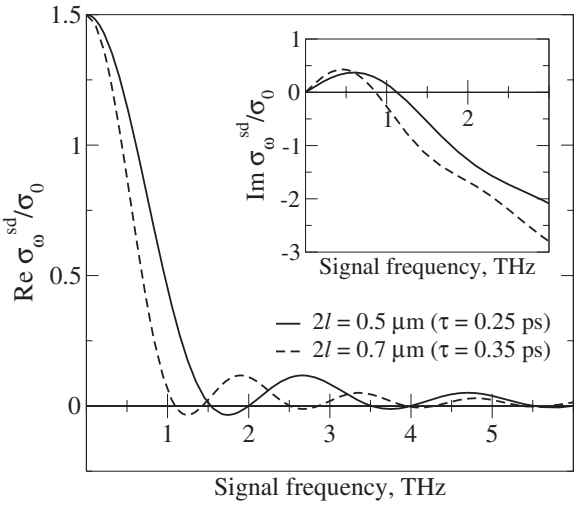

Fig. 2. Real part and imaginary part (inset) of the ac conductance σ_ω^{sd} as functions of signal frequency $f = \omega/2\pi$ for different lengths of i-section (different transit times).

frequency ranges where it has different signs. The frequency dependence of the imaginary part corresponds to the domination of the inductive component at low frequencies (associated with the contribution of electrons and holes) and the capacitive component at elevated frequencies (due to the contribution of the geometrical capacitance). The relative value of the real part of the ac conductance at the first minimum at $2l = 0.5\,\mu$m is fairly moderate: $\mathrm{Re}\,\sigma^{sd}_{\omega=2\pi f_1}/\sigma_0 \simeq -0.034$. However, it is larger than that in some new concept THz devices.[27] Considering the above estimate of σ_0 at $V_0 = 0.1 - 1\,$V, one can obtain $\mathrm{Re}\,\sigma^{sd}_{\omega=2\pi f_1} \simeq -(7-24)\,$mS/mm (at $f_1 \simeq 1.7\,$THz). For a G-TUNNETT with the top gate width $H = 100\,\mu$m, which is typical for high-electron mobility transistors (HEMTs), one obtains $Y = \mathrm{Re}\,\sigma^{sd}_{\omega=2\pi f_1} H \simeq -(0.7-2.4)\,$mS. These values are somewhat smaller than those calculated for resonant-tunneling diodes (RTDs)[28] with rather short transit region: $Y = \mathrm{Re}\,\sigma^{sd}_{\omega=2\pi f_1} H \lesssim -10\,$mS for an RTD with the area $1.8 \times 1.8\,\mu\mathrm{m}^2$ and $f_1 \simeq 1.7\,$THz). It worth noting that due to the lateral structure and relatively large spacing between the top gates and, hence, highly conducting p- and n-sections, i.e., long i-section (which is allowed owing to fairly high electron and hole directed velocities in G-TUNNETTs), the G-TUNNETT capacitance C can be much smaller than the gate capacitance of HEMTs C^{HEMT}. Indeed, $C/C^{HEMT} \simeq 2\Lambda\, W_g/\pi\, L_g \ll 1$ (for the same width H), where Λ is a logarithmic factor on the order of unity,[29] whereas W_g and $L_g \gg W_g$ are the HEMT gate layer thickness and gate length, respectively. Further increase in $|\mathrm{Re}\,\sigma^{sd}_{\omega=2\pi f_1}|$ and f_1 can be achieved by using shorter i-sections and higher bias source–drain voltages because $\mathrm{Re}\,\sigma_\omega \propto V_0^{3/2}/l^{1/2}$ and $f_1 \propto l^{-1}$. The nonuniformity of the electric field in the i-section[22] resulting in its elevated values near the edges of the i-section can also give rise to a significant increase in the dc current and, consequently, leading to an increase in $|\mathrm{Re}\,\sigma^{sd}_{\omega=2\pi f_1}|$. However, the consideration of the high-voltage operation and accounting for the effects of the electric field nonuniformity add significant complexity to the device model.

As follows from the above estimates and Fig. 2, the negativity of the real part of the ac conductance at the frequencies $f > 1\,$THz can be achieved in the G-TUNNETT structures with the i-section length only moderately smaller than one micrometer.

In conclusion, we have proposed a G-TUNNETT and calculated its ac conductance as a function of the signal frequency and the structural parameter using the developed device model. We have demonstrated that the ac conductance exhibits the frequency ranges where it is negative. Due to high directed energy independent velocities of the electrons and holes generated owing to the interband tunneling, these frequency regions correspond to the THz range at relatively large length of the i-region. A G-TUNNETT can work as an active element of THz oscillators with a complementary resonant cavity.

Acknowledgments The authors are grateful to Professor T. Otsuji for stimulating discussions. The work was supported by the Japan Science and Technology Agency, CREST and by a Grant-in-Aid for Scientific Research (S) from the Japan Society for the Promotion of Science. The work was also partially supported by the Airforce Office of Scientific Research, U.S.A.

1) C. Berger *et al.*: J. Phys. Chem. **108** (2004) 19912.
2) K. S. Novoselov *et al.*: Nature **438** (2005) 197.
3) A. K. Geim and K. S. Novoselov: Nat. Mater. **6** (2007) 183.
4) J. Hass *et al.*: Appl. Phys. Lett. **89** (2006) 143106.
5) V. V. Cheianov and V. I. Fal'ko: Phys. Rev. B **74** (2006) 041403.
6) B. Huard *et al.*: Phys. Rev. Lett. **98** (2007) 236803.
7) B. Ozyilmaz *et al.*: Phys. Rev. Lett. **99** (2007) 166804.
8) V. Ryzhii *et al.*: Appl. Phys. Express **1** (2008) 013001.
9) V. Ryzhii *et al.*: Phys. Status Solidi A **205** (2008) 1527.
10) B. Obradovic *et al.*: Appl. Phys. Lett. **88** (2006) 142102.
11) Z. Chen *et al.*: Physica E **40** (2007) 228.
12) Y. Quyang *et al.*: Appl. Phys. Lett. **89** (2006) 203107.
13) V. Ryzhii *et al.*: J. Appl. Phys. **103** (2008) 094510.
14) V. Ryzhii *et al.*: Appl. Phys. Express **1** (2008) 063002.
15) E. McCann: Phys. Rev. B **74** (2006) 161403.
16) E. V. Castro *et al.*: Phys. Rev. Lett. **99** (2007) 216802.
17) S. V. Morozov *et al.*: Phys. Rev. Lett. **100** (2008) 016602.
18) Xu Du *et al.*: Nat. Nanotechnol. **3** (2008) 491.
19) G. I. Haddad and R. J. Trew: IEEE Trans. Microwave Theory Tech. **50** (2002) 760.
20) Z. S. Gribnikov *et al.*: J. Appl. Phys. **93** (2003) 5435.
21) L. M. Zhang and M. M. Fogler: Phys. Rev. Lett. **100** (2008) 116804.
22) M. M. Fogler *et al.*: Phys. Rev. B **77** (2008) 075420.
23) W. Shockley: J. Appl. Phys. **9** (1938) 635.
24) S. Ramo: Proc. IRE **27** (1939) 584.
25) V. Ryzhii and G. Khrenov: IEEE Trans. Electron Devices **42** (1995) 166.
26) V. Ryzhii *et al.*: J. Phys.: Conf. Ser. **38** (2006) 228.
27) V. N. Sokolov *et al.*: Appl. Phys. Lett. **90** (2007) 142117.
28) M. Asada *et al.*: Jpn. J. Appl. Phys. **47** (2008) 4375.
29) V. Ryzhii *et al.*: J. Phys.: Conf. Ser. **38** (2006) 228.